



## Dynamic Exchange Controls the Assembly Structure of Nucleic-Acid-Peptide Chimeras

Journal:	<i>Soft Matter</i>
Manuscript ID	SM-ART-11-2022-001528.R1
Article Type:	Paper
Date Submitted by the Author:	13-May-2023
Complete List of Authors:	Sadihov-Hanoch, Hava; Ben Gurion University of the Negev, Department of Chemistry Bandela, Anil Kumar; Ben Gurion University of the Negev, Department of Chemistry Chotera, Agata; Ben Gurion University of Negev, Department of Chemistry Ben David, Oshrat; Ben Gurion University of the Negev, Department of Chemistry Cohen-Luria, Rivka; Ben Gurion University of the Negev, Department of Chemistry Lynn, David; Emory University, Ashkenasy, Gonen; Ben Gurion University of the Negev, Department of Chemistry

## ARTICLE

## Dynamic Exchange Controls the Assembly Structure of Nucleic-Acid-Peptide Chimeras

Received 00th January 20xx,  
Accepted 00th January 20xx

Hava Sadihov-Hanoch,<sup>a</sup> Anil Kumar Bandela,<sup>a</sup> Agata Chotera-Ouda,<sup>a,b</sup> Oshrat Ben David,<sup>a</sup> Rivka Cohen-Luria,<sup>a</sup> David G. Lynn<sup>c</sup> and Gonen Ashkenasy\*<sup>a</sup>

DOI: 10.1039/x0xx00000x

Recent attempts to develop the next generation of functional biomaterials focus on systems chemistry approaches exploiting dynamic networks of hybrid molecules. This task is often found challenging, but we herein present ways for profiting from the multiple interaction interfaces forming Nucleic-acid-Peptide assemblies and tuning their formation. We demonstrate that the formation of well-defined structures by double-stranded DNA-peptide conjugates (dsCon) is restricted to a specific range of environmental conditions and that precise DNA hybridization, satisfying the interaction interfaces, is a crucial factor in this process. We further reveal the impact of external stimuli, such as competing free DNA elements or salt additives, which initiate dynamic interconversions, resulting in hybrid structures exhibiting spherical and fibrillar domains or a mixture of spherical and fibrillar particles. This extensive analysis of the co-assembly systems chemistry offers new insights into prebiotic hybrid assemblies that may now facilitate the design of new functional materials. We discuss the implications of these findings for the emergence of function in synthetic materials and during early chemical evolution.

### Introduction

Current evolved interactions between nucleic acids (NAs) and proteins confer remarkable control over cellular function. Among the best characterized complexes are the nucleosomes engaging in DNA packaging in eukaryotes, ribosomes that translate RNA sequences into specific proteins, ribonucleoprotein granules in RNA processing, and amino-acid-charged *t*-RNAs exploited in translation.<sup>[1]</sup> Based on the structure-function relations in these complexes, several groups (including the authors) proposed that the preparation of synthetic nucleic-acid-peptide (NA-pep) hybrid materials might be exploited for applications in bio-nanotechnology.<sup>[2]</sup> Systems Chemistry approaches to the chemical origins of NA-pep assemblies continue to reveal now NA-pep functionality.<sup>[3]</sup> Recent investigations have, for example, demonstrated that (i) DNA sequences can template amyloids formation,<sup>[4]</sup> (ii) interactions between proto-peptides and RNA cooperatively stabilize both species,<sup>[5]</sup> and (iii) short nucleobase peptide chimeras can replicate through autocatalysis and cross catalysis.<sup>[6]</sup>

While self-organizing systems based separately on NA and peptides have been extensively explored,<sup>[7]</sup> studies on the self-assembly of NA-pep chimeras were only initiated in recent years.<sup>[8]</sup> These assays revealed that the NA-pep assembly can provide access to new architectures, but at the same time that it is difficult to predict and control the outputs, since complex web of interactions govern the kinetics and thermodynamics of such processes.<sup>[2h, i, 6b, 9]</sup> Accordingly,

we have systematically developed reversible self-assembly reactions to tune the formation of NA-pep materials and to find ways for satisfying the multiple interaction interfaces affecting the assembly structures. The comprehensive investigation of the co-assembly structure and dynamics yields new insight into prebiotic hybrid complexes. It may therefore enhance the development of new functional materials with adapted properties and functions.

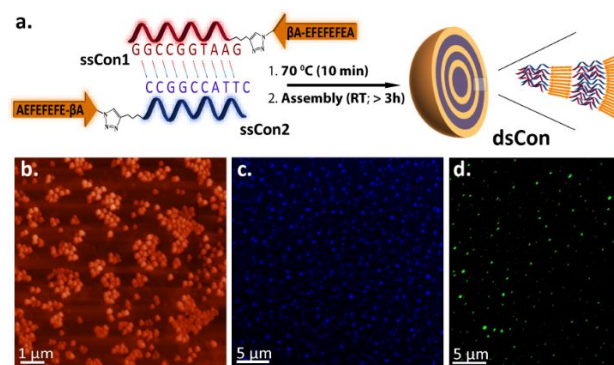


**Fig. 1** Assembly structure of the dsCon chimeras. (a) Hybridization of single strand conjugates (ssCon1 and ssCon2; see characterization in Figs. s1, s2.) and their assembly to multi lamellar spheres (dsCon). The single-letter nomenclature is used to represent the DNA and peptide sequences (BA =  $\beta$ -alanine). For specific names and sequences see also Table s1. (b) AFM image of the dsCon particles. (c,d) Fluorescence microscopy images of the dsCon stained with (2.8  $\mu$ M) DAPI and (100  $\mu$ M) ThT, respectively. In all experiments, [ssCon1] = [ssCon2] = 25  $\mu$ M, [MgCl<sub>2</sub>] = 10 mM in phosphate buffer pH=7.

### Results and discussion

We started by mixing and annealing two complementary single strand NA-pep conjugates (ssCon1 and ssCon2; Fig. 1) that co-

<sup>a</sup> Address here.

<sup>b</sup> Address here.

<sup>c</sup> Address here.

† Footnotes relating to the title and/or authors should appear here.

Electronic Supplementary Information (ESI) available: [details of any supplementary information available should be included here]. See DOI: 10.1039/x0xx00000x

assemble into a multi-lamellar, onion-like structure (dsCon; Fig. 1). In these spherical objects, the amphiphilic peptide tails form anti-parallel  $\beta$ -sheet patches,<sup>[10]</sup> while the DNA segments hybridize with each other (Fig. 1a).<sup>[2f]</sup> Since both the peptide and DNA segments are negatively charged, electrostatic repulsion prevents their interactions with each other. Using spectroscopy and microscopy assays, we show that the dsCon well-defined structure only forms under a narrow set of environmental conditions, and that satisfying the interaction interfaces by perfect DNA hybridization is key to this process. Furthermore, we demonstrate how external cues, such as a competing free DNA segment or salt additives, lead to dynamic interconversion, forming mixed structures with spherical and fibrillar domains or mixtures containing both spherical and fibrillar particles. The dsCon assembly structure (Fig. 1a) was characterized by transmission electron microscopy (TEM), atomic force microscopy (AFM) and fluorescence microscopy. The TEM and AFM results clearly show that the conjugates assemble into spheres (Figs. 1b, 4a and s3 in SI) with diameters ranging 20–180 nm.<sup>[2f]</sup> Bright field fluorescence microscopy images revealed spherical objects (Fig. s4) that could be stained with either 4',6-diamidino-2-phenylindole (DAPI), that binds strongly to adenine–thymine-rich regions in dsDNA, or Thioflavin T (ThT), that typically binds to peptide  $\beta$ -sheets. The stained structures emitted light from both the dyes, i.e., blue fluorescence for excitation of DAPI and green fluorescence for ThT (Fig. 1c,d), supporting both DNA hybridization and  $\beta$ -sheet formation within the assembled structures as shown in Figure 1a.

Remarkably, by circular dichroism (CD) we observed that upon formation of the lamellar structures, the double-stranded DNA segments of the conjugates undergo conformational changes (Fig. 2, and Figs. s6, and s8). Figure 2a presents the dsCon spectrum in *black* with additional curves representing signal deconvolution. The spectral minimum at 216 nm relates to the peptide  $\beta$ -sheets<sup>[11]</sup> while the minimum at  $\sim$ 210 nm and maximum at 260 nm are consistent with the DNA A-conformation, and the minimum at 240 nm and maximum at 280 nm suggest B-DNA structure.<sup>[12]</sup> The control experiments with the dsDNA alone or (non-conjugated) dsDNA + p9 solutions carried out under the same conditions only show signals originating from the A-conformation (Fig. 2c, d). A-DNA helix structure is typically observed for short GC-rich sequences and is stabilized by low hydration. We propose that upon formation of the dsCon assembly, the DNA segments transform to the more densely packed B-form. This conformation is potentially more symmetrical in its organization (Fig. 2a inset) that is highly hydrated due to conjugation with the amphiphilic peptide segments. In living cells, DNA is often found as a mixture of A- and B-conformations, and the transitions of one form to the other take place during specific cellular functions.<sup>[13]</sup> In the present context, the two DNA conformations might change from one to the other upon changing the environmental conditions, facilitating the formation of various forms of hybrid materials with different topologies (*vide infra*), and potentially, with different functional significance.

The formation of highly ordered dsCon spherical nanoparticles was found to be robust and reproducible under the conditions depicted in Figure 1. We have therefore considered this set of conditions as 'ideal' and proceeded to characterize the stability and dynamics of various modifications. Two experimental vectors were first considered, featuring the addition of increasing amounts of ssDNA

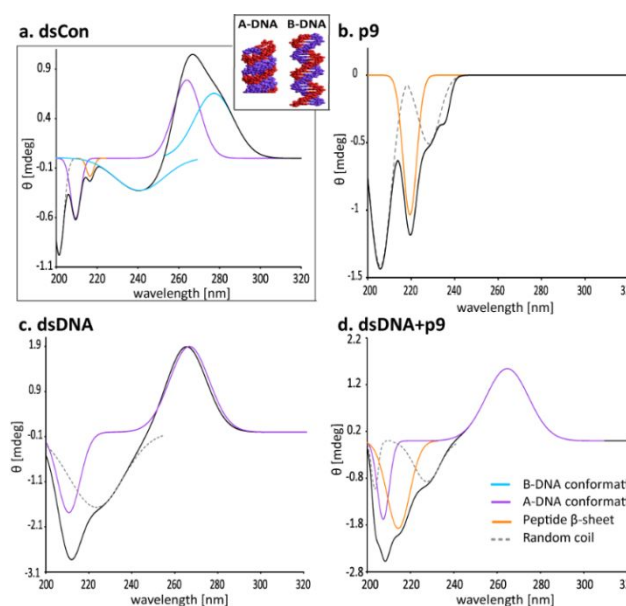


**Fig. 2** CD based analysis of the DNA and peptide secondary structures in dsCon and related assemblies. (a) dsCon; (b) p9 peptide (azide-modified peptide segment, synthesis precursor of the ssCon); (c) dsDNA (d) dsDNA and p9 peptide mixture. Concentrations of all samples was 10  $\mu$ M in 10 mM phosphate buffer pH 7. Deconvolution analysis of the CD spectra achieved based on the typical spectra of B-DNA, A-DNA, peptide  $\beta$ -sheet and random coils. Additional details are given in SI Section s3a and Table s2.

(DNA1) suitable for competing with ssCon1 in binding to ssCon2, possibly interfering with the assembly process and leading to alternative architectures. The first system involved mixing the two ssCon and DNA1 at *time* = 0 and following their simultaneous co-assembly for 4h (Fig. 3 *left*). Co-assembly of the second system took place through strand exchange, achieved by first equilibrating the dsCon for 1h to form the spheres (Fig. s5) and then incubating with DNA1 for the subsequent 3h (Fig. 3 *right*, details in SI supplementary methods).

For the simultaneous co-assembly, we observed that the addition of 10% of DNA1 (molar ratio vs. ssCon1 or ssCon2) yielded both fibrillar and spherical structures (Fig. 3a), whereas mixing with 50% or 150% DNA1 led to fibers only (Fig. 3c,e). CD spectra of co-assembly with 10%, 25% and 50% addition of DNA1 showed the formation of  $\beta$ -sheet, as well as A and B dsDNA, supporting the fact that ssDNA at a low molar ratio can hinder assembly into spheres. Based on the CD data deconvolution, we propose that the B-DNA conformation population decreased with the increase of DNA1 molar ratio (Fig. s6 and Table s3). For higher DNA1 molar ratio (150%), the CD spectrum showed the formation of  $\beta$ -sheet and a lower percentage of B-DNA versus the other samples, as well as significant minimum at 230 nm (Fig. s6b), indicating that excess ssDNA encourages assembly of fiber and (up to 42%) random coil architectures.

In the strand exchange experiments, adding the DNA1 at low concentrations (10% and 50%) to the mixture of pre-assembled dsCon did not alter their spherical structure (Fig. 3b, d), but the addition of excess DNA1 (150%) induced a conformational change into short, branched fibers (Fig. 3f and Table s4). These experiments demonstrated that the DNA segments of the dsCon can arrange themselves to give stable assemblies but also disassemble upon addition of excess competitor DNA1. In competitive co-assembly,

strong competition for binding ssCon2 prevents assembly into spheres. Alternatively, the strand exchange experiments reveal that the spheres which are formed within 1h are already kinetically stable and could only be disassembled in presence of excess DNA1 during relatively long incubation times (3h). For both systems we argue that the formation of fibers is facilitated by the peptide segments of the conjugates, while the DNA segments remain exposed at the periphery of the supramolecular structure and engage in hybridization with the competitive DNA1 strand (see scheme below; Fig. 5, Entry 8 pink panel).

Since the extent of DNA hybridization and the formation of dsDNA secondary structures can be influenced by electrostatic forces in their vicinity,<sup>[4]</sup> we have further studied the effect of adding various (divalent and monovalent) metal cations on the dsCon rearrangement and assembly structures (TEM/AFM Fig. 4 and CD Fig. s8). As specified above (Fig. 1), the ideal conditions for the assembly of dsCon into the stable spherical architecture included the addition

of 10 mM MgCl<sub>2</sub> (Figs. 4a and s8a). When no metal ions were added, the dsCon primarily assembled into (micrometer long) fibers, with only a small number of spheres co-existing (Fig. 4b). Assembly in the presence of a lower amount of MgCl<sub>2</sub> (5 mM) probably stabilized DNA hybridization to a lower extent (than 10 mM), as evident by coexistence of particles having both the sphere and fiber topologies (Fig. 4c). The addition of 10 mM CaCl<sub>2</sub> led to yet another morphology, i.e., shorter fibers, ca. 110 nm in length (Figs. 4d and s8a; Table s3). This finding could be explained by that the Ca<sup>2+</sup> ions have stronger affinity to the peptide Glu carboxylic acids (than Mg<sup>2+</sup>),<sup>[14]</sup> and generally by previous evidence that Ca<sup>2+</sup> ions can induce a transition from B- to a non-B-DNA conformation,<sup>[15]</sup> hence lowering the propensity for forming the dsCon spheres. We further observed that the addition of monovalent cations (20 mM LiCl or NaCl), which do not stabilize the DNA backbone like Mg<sup>2+</sup>, yielded mixtures of fibers and spheres (Figs. 4e,f and s8a).

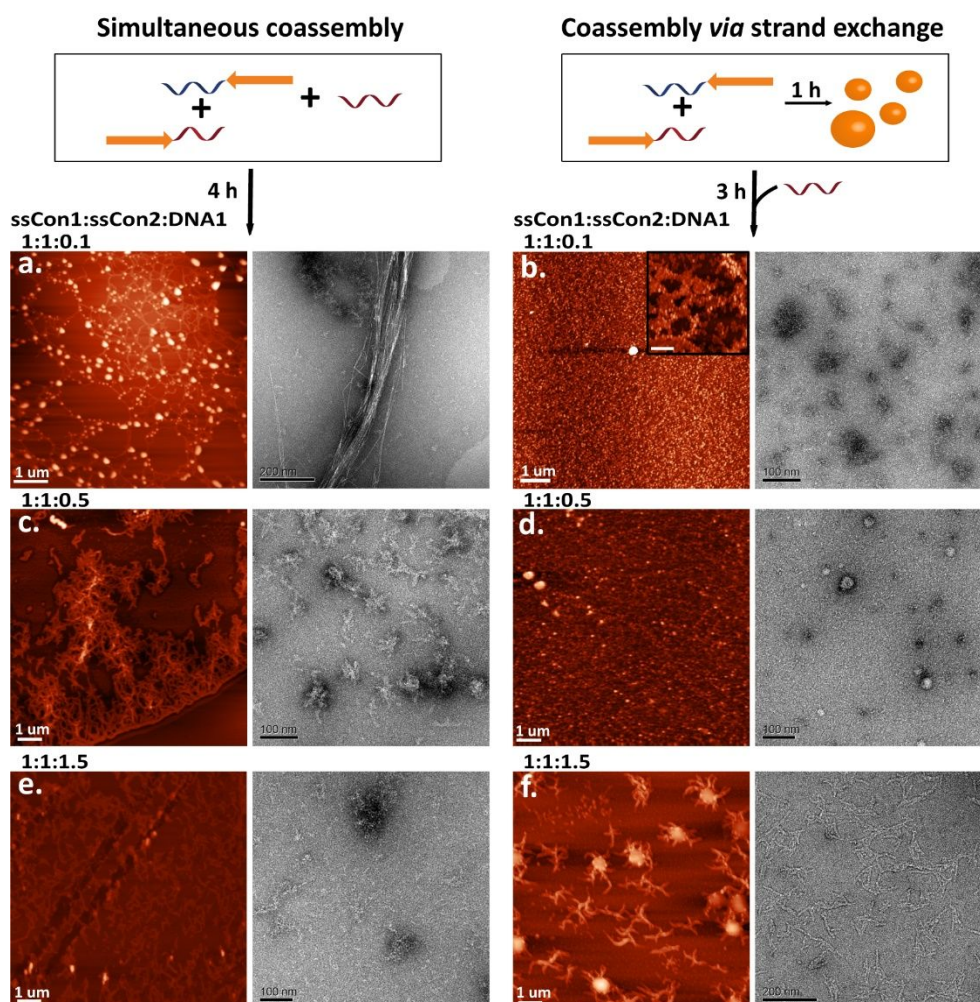


**Fig. 3** dsCon co-assembly in the presence of the free ssDNA, DNA1. AFM and TEM images of nanostructures formed in mixtures containing ssCon1, ssCon2 and DNA1 at variable ratios, and after different times of equilibration. (a, c, e) Images obtained for samples in which DNA1 added together with ssCon1 and ssCon2. (b, d, f) Images obtained for samples in which DNA1 was added after 1h pre-equilibration of ssCon1 and ssCon2, *insert to b* – an AFM image of a different scanned area showing a lower density of spherical objects. All the experiments [ssCon1] = [ssCon2] = 25  $\mu$ M, [MgCl<sub>2</sub>] = 10 mM in phosphate buffer pH=7.

## COMMUNICATION

Temperature dependent denaturation experiments (following the absorbance at 260 nm; Fig. s9) for the dsCon assembly in the presence of different metal cations indicated only one transition in all cases, accounted for the structural changes from the double stranded DNA to a single strand DNA. The analysis further revealed higher  $T_m$  values for the stable assemblies formed in the presence of  $Mg^{2+}$  ions, in comparison to those formed in the presence of monovalent cations (LiCl, NaCl). Additionally, based on CD characterization of the p9 peptide assembly in the presence of different metal ions (Fig. s8b), we can conclude that these ions (except for  $Ca^{2+}$ ) do not interact strongly with the peptide residues, since in all cases the spectra suggested a similar  $\beta$ -sheet secondary arrangement. Interestingly, in several cases where both the spheres and fibers formed, we noticed that particles of different morphologies were closely attached, forming branched superstructures or 'necklaces' (Inserts to Fig. 4b,c,f, Fig. 5 and Figs. s7, s10). We suggest that in those cases the spheres were attached to the fibers through hybridization of loose DNA tails present on edges of both assemblies.

### Conclusions

The plethora of supramolecular structures formed by NA-pep conjugates are summarized in Table 1 and Figure 5, displaying the structural models for the morphologies produced through direct assembly of the ssCon chimeras, and when assembled individually,<sup>[2f]</sup> in or the presence of competing peptide<sup>[2f]</sup> or DNA molecules. Our former study has shown how the conjugation (of peptide and DNA segments) improves the assembly properties, i.e., stability and binding affinity, versus the assemblies of each segment alone.<sup>[2f]</sup> Notably, the adaptivity of the system to changes in the environment caused liquid-liquid phase separation and the appearance of transient liquid droplet condensates (Fig. s11), as has been observed for other complex mixtures of biological molecules.<sup>[4, 16]</sup> These features will be further characterized in our next studies. Both peptide and nucleic acid precursors may be formed in prebiotic environments from simple building blocks of unified origin,<sup>[3a]</sup> so we suggest that harnessing the synergistic activity of peptide and nucleic acid with the chemical cues applied here may have led to the selection of functional chimeras. Since synergy was also observed for related prebiotically-relevant molecules,<sup>[17]</sup> such as NA-lipid,<sup>[18]</sup> pep-lipid,<sup>[19]</sup> and carbohydrate-pep,<sup>[20]</sup> our study underscores how rapid progression in complexity and systems chemistry<sup>[21]</sup> could now provide access to a large repertoire of functional co-assemblies.

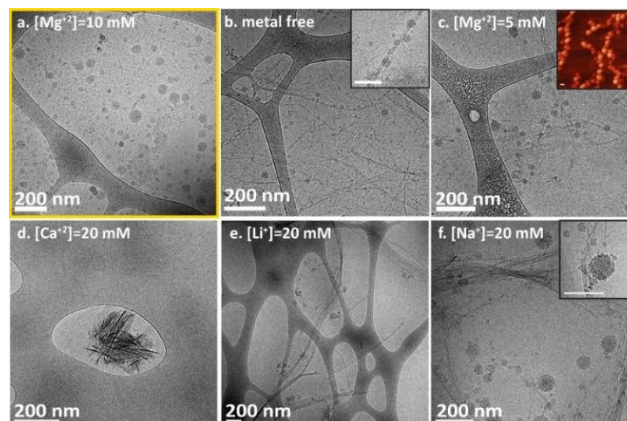


**Fig. 4** Cryo-TEM images of self-assembled nanostructures formed in mixtures containing (250  $\mu$ M each) ssCon1 and ssCon2 in the presence of different metal ions, in phosphate buffer pH=7. (a) dsCon;  $Mg^{2+}$  (10 mM); (b) control experiment: dsCon without metal ions; (c) dsCon;  $Mg^{2+}$  (5 mM); (d) dsCon;  $Ca^{2+}$  (10 mM); (e) dsCon;  $Li^+$  (20 mM); (f) dsCon;  $Na^+$  (20 mM).

### Acknowledgements

Funding was provided by an NSF-BSF grant (NSF: DMR-2004846; BSF: 2019745) and by the Horizon 2020 FET Open (G.A.; CLASSY project, Grant Agreement N° 862081). H.S.H. and A.K.B. received support from the BGU Kreitmann fellowships program.

### Author Contributions

H.S.H., D.G.L. and G.A. conceptualized the research; H.S.H., A.K.B., A.C.O. and O.B-D. conducted the research, including data acquisition and analysis. All authors read and comment on the manuscript.

### Conflicts of interest

There are no conflicts to declare.

Table 1 Assembly structures observed for dsCon and related mixtures under variable conditions					
Entry #	ssCon1: ssCon2 <sup>a</sup>	Additives <sup>a,b,c</sup>		Observed morphology	Analytical tools
		Seq (eq.)	Salt (mM)		
<b>Self-assembly of the p9 peptide and dsCon</b>					
1	-	P9		Fibers	AFM, CD c-TEM,
2	1:1	-	MgCl <sub>2</sub> (10)	Spheres, LD	AFM, FM, TEM, CD c-TEM,
<b>Dynamic exchange in presence of ssDNA</b>					
3	1:1	DNA1 (0.1) <sup>b</sup>	MgCl <sub>2</sub> (10)	Spheres, fibers	AFM, TEM
4	1:1	DNA1 (0.1) <sup>c</sup>	MgCl <sub>2</sub> (10)	Spheres	AFM, TEM
5	1:1	DNA1 (0.5) <sup>b</sup>	MgCl <sub>2</sub> (10)	Fibers	AFM, TEM
6	1:1	DNA1 (0.5) <sup>c</sup>	MgCl <sub>2</sub> (10)	Spheres	AFM, TEM
7	1:1	DNA1 (1.5) <sup>b</sup>	MgCl <sub>2</sub> (10)	Fibers	AFM, TEM
8	1:1	DNA1 (1.5) <sup>c</sup>	MgCl <sub>2</sub> (10)	Fibers	AFM, TEM
<b>Self-assembly in presence of metal ions</b>					
9	1:1	-	None	Fibers, spheres, LD	AFM, c-TEM
10	1:1	-	MgCl <sub>2</sub> (5)	Spheres, fibers, LD	AFM, c-TEM
11	1:1	-	CaCl <sub>2</sub> (10)	Short fibers	c-TEM
12	1:1	-	NaCl (20)	Spheres, fibers, LD	c-TEM
13	1:1	-	LiCl (20)	Spheres, fibers, LD	AFM, c-TEM
<b>Mixing p9 peptide with increasing amounts of DNA-pep chimeras<sup>[2f]</sup></b>					
14	1:0	-	-	Fibers, LD	AFM, c-TEM
15	1:0	P9 (1)	MgCl <sub>2</sub> (10)	Fibers, LD	AFM
16	1:1	P9 (8)	MgCl <sub>2</sub> (10)	Fibers, spheres	AFM
17	1:1	P9 (1)	MgCl <sub>2</sub> (10)	Spheres, fibers, LD	AFM, c-TEM

<sup>a</sup>The additives actual concentrations in each experiment are given in the respective figure captions and SI experimental sections; <sup>b</sup>DNA1 co-assembled with ssCon1 and ssCon2 from time = 0; <sup>c</sup>DNA1 added into the mixture of ssCon1 and ssCon2 after the latter were allowed to equilibrate for 1h. LD = liquid droplets; FM = fluorescence microscopy; c-TEM = cryo-TEM.

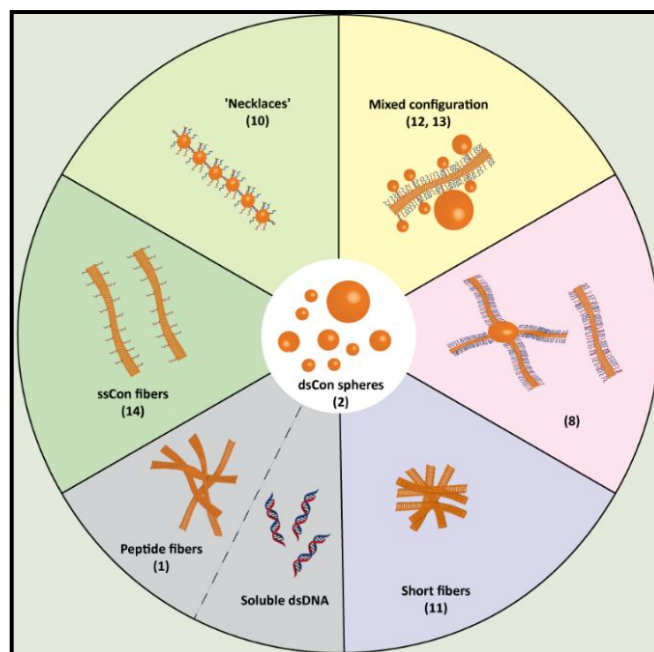


Fig. 5 Schematic representation the different topologies obtained for dsCon and related mixtures under variable conditions. Entry numbers matched with Table 1.

## Notes and references

- 1 a) A. Yonath, *Angew. Chem., Int. Ed.* 2010, **49**, 4340; b) K. Y. Sanbonmatsu, *Curr. Opin. Struct. Biol.* 2019, **55**, 104; c) J. D. Perlmutter and M. F. Hagan, *Annu. Rev. Phys. Chem.* 2015, **66**, 217; d) J. C. Bowman, A. S. Petrov, M. Frenkel-Pinter, P. I. Penev and L. D. Williams, *Chem. Rev.* 2020, **120**, 4848.
- 2 a) R. Freeman, M. Han, Z. Álvarez, J. A. Lewis, J. R. Wester, N. Stephanopoulos, M. T. McClendon, C. Lynsky, J. M. Godbe, H. Sangji, E. Luijten and S. I. Stupp, *Science* 2018, **362**, 808; b) R. Chang, E. Nikoloudakis, Q. Zou, A. Mitraki, A. G. Coutsolelos and X. Yan, *ACS Appl. Bio. Mater.* 2019, **3**, 2; c) I. M. Gabas and P. E. Nielsen, *Biomacromolecules* 2020, **21**, 472; d) A. Buchberger, C. R. Simmons, N. E. Fahmi, R. Freeman and N. Stephanopoulos, *J. Am. Chem. Soc.* 2020, **142**, 1406; e) C. S. Swenson, A. Velusamy, H. S. Argueta-Gonzalez and J. M. Heemstra, *J. Am. Chem. Soc.* 2019, **141**, 19038; f) A. Chotera, H. Sadihov, R. Cohen-Luria, P. A. Monnard and G. Ashkenasy, *Chem. Eur. J.* 2018, **24**, 10128; g) N. Stephanopoulos, *Bioconjugate Chem.* 2019, **30**, 1915; h) M. Kye and Y. Lim, *Angew. Chem. Int. Ed.* 2016, **55**, 12003; i) R. Ni and Y. Chau, *J. Am. Chem. Soc.* 2014, **136**, 17902; j) A. D. Merg, R. V. Thanner, S. Mokashi-Punekar, S. T. Nguyen and N. L. Rosi, *Chem. Commun.* 2017, **53**; k) B. Liu, C. G. Pappas, E. Zangrando, N. Demitri, P. J. Chmielewski and S. Otto, *J. Am. Chem. Soc.* 2019, **141**, 1685.
- 3 a) B. H. Patel, C. Percivalle, D. J. Ritson, C. D. Duffy and J. D. Sutherland, *Nat. Chem.* 2015, **7**, 301; b) Y. Bai, A. Chotera, O. Taran, C. Liang, G. Ashkenasy and D. G. Lynn, *Chem. Soc. Rev.* 2018, **47**, 5444; c) B. Jash, P. Tremmel, D. Jovanovic and C. Richert, *Nat. Chem.* 2021, **13**, 751.
- 4 A. K. Rha, D. Das, O. Taran, Y. Ke, A. K. Mehta and D. G. Lynn, *Angew. Chem. Int. Ed.* 2020, **59**, 358.
- 5 M. Frenkel-Pinter, J. W. Haynes, A. M. Mohyeldin, M. C. A. B. Sargon, A. S. Petrov, R. Krishnamurthy, N. V. Hud, L. D. Williams and L. J. Leman, *Nat. Commun.* 2020, **11**, 3137.
- 6 a) B. Liu, C. G. Pappas, J. Ottele, G. Schaeffer, C. Jurissek, P. F. Pieters, M. Altay, I. Maric, M. C. A. Stuart and S. Otto, *J. Am. Chem. Soc.* 2020, **142**, 4184; b) A. K. Bandela, N. Wagner, H. Sadihov, S. Morales-Reina, A. Chotera-Ouda, K. Basu, R. Cohen-Luria, A. de la Escosura and G. Ashkenasy, *Proc. Natl. Acad. Sci. U. S. A.* 2021, **118**, e2015285118.
- 7 a) S. Cavalli, F. Albericio and A. Kros, *Chem. Soc. Rev.* 2010, **39**, 241; b) C. D. Spicer, C. Jumeaux, B. Gupta and M. M. Stevens, *Chem. Soc. Rev.* 2018, **47**, 3574; c) M. Amit, S. Yuran, E. Gazit, M. Reches and N. Ashkenasy, *Adv. Mater.* 2018, **30**, 1707083; d) A. Lampel, *Chem* 2020, **6**, 1222; e) M. Frenkel-

- Pinter, M. Samanta, G. Ashkenasy and L. J. Leman, *Chem. Rev.* 2020, **11**, 4707; f) S. Fan, D. Wang, A. Kenaan, J. Cheng, D. Cui and J. Song, *Small* 2019, **15**, 1805554; g) Y. Dong, C. Yao, Y. Zhu, L. Yang, D. Luo and D. Yang, *Chem. Rev.* 2020, **120**, 9420.
- 8 A. Kumar Bandela, H. Sadihov-Hanoch, R. Cohen-Luria, C. Gordon, A. Blake, G. Poppitz, D. G. Lynn and G. Ashkenasy, *Israel Journal of Chemistry* 2022, **62**, e202200030.
- 9 C. Suparpprom and T. Vilaivan, *RSC Chemical Biology* 2022, **3**, 648.
- 10 Y. Raz, B. Rubinov, M. Matmor, H. Rapaport, G. Ashkenasy and Y. Miller, *Chem. Commun.* 2013, **49**, 6561.
- 11 J. Nanda, B. Rubinov, D. Ivnitski, R. Mukherjee, E. Shtelman, Y. Motro, Y. Miller, N. Wagner, R. Cohen-Luria and G. Ashkenasy, *Nat. Commun.* 2017, **8**, 434.
- 12 J. Kypr, I. Kejnovska, D. Renciuik and M. Vorlickova, *Nucleic Acids Res.* 2009, **37**, 1713.
- 13 D. W. Ussery, *DNA Structure: A-, B- and Z-DNA Helix Families*, *Encyclopedia of Life Sciences*, John Wiley & Sons Ltd, Chichester, U.K. 2002.
- 14 a) R. Zou, Q. Wang, J. Wu, J. Wu, C. Schmuck and H. Tian, *Chemical Society Reviews* 2015, **44**, 5200; b) I. W. Hamley, *Soft Matter* 2011, **7**, 4122.
- 15 A. Dobi and D. V. Agoston, *Proc. Natl. Acad. Sci. USA* 1998, **95**, 5981.
- 16 R. R. Poudyal, R. M. Guth-Metzler, A. J. Veenis, E. A. Frankel, C. D. Keating and P. C. Bevilacqua, *Nat. Commun.* 2019, **10**, 490.
- 17 Y. M. Abul-Hajja, G. G. Scott, J. K. Sahoo, T. Tuttle and R. V. Ulijn, *Chem. Commun.* 2017, **53**, 9562.
- 18 a) R. S. Shirazi, K. K. Ewert, B. F. B. Silva, C. Leal, Y. Li and C. R. Safinya, *Langmuir* 2012, **28**, 10495; b) M. C. Wamberg, R. Wieczorek, S. B. Brier, J. W. d. Vries, M. Kwak, A. Herrmann and P.-A. Monnard, *Bioconjugate Chem.* 2014, **25**, 1678–1688; c) S. Morales-Reina, C. Giri, M. Leclercq, S. Vela-Gallego, I. de la Torre, J. R. Castón, M. Surin and A. de la Escosura, *Chem. Eur. J.* 2020, **26**, 1082.
- 19 a) S. Murillo-Sanchez, D. Beaufils, J. M. Gonzalez Manas, R. Pascal and K. Ruiz-Mirazo, *Chem. Sci.* 2016, **7**, 3406; b) E. C. Izgu, B. A., N. P. Kamat, V. S. Lelyveld, W. Zhang, T. Z. Jia and J. W. Szostak, *J. Am. Chem. Soc.* 2016, **138**, 16669; c) H. R. Marsden, I. Tomatsu and A. Kros, *Chem. Soc. Rev.* 2011, **40**, 1572.
- 20 a) A. J. Wagner, D. Y. Zubarev, A. Aspuru-Guzik and D. G. Blackmond, *ACS Cent. Sci.* 2017, **3**, 322; b) A. Brito, Y. M. Abul-Hajja, D. S. da Costa, R. Novoa-Carballal, R. L. Reis, R. V. Ulijn, R. A. Pires and I. Pashkuleva, *Chem. Sci.* 2019, **10**, 2385.
- 21 a) G. Ashkenasy, T. M. Hermans, S. Otto and A. F. Taylor, *Chem. Soc. Rev.* 2017, **46**, 2543; b) D. Kroiss, G. Ashkenasy, A. B. Braunschweig, T. Tuttle and R. V. Ulijn, *Chem* 2019, **5**, 1917.